3D characterization of defects in Guided Wave monitoring of pipework using a magnetostrictive sensor

Francesco Bertoncini, Constantin Oprea, Marco Raugi, Florin Turcu
Department of Electrical Systems and Automation - University of Pisa, Italy
Phone: +39 050 2217300, Fax: +39 050 2217333; e-mail: {bertoncini, oprea, raugi, turcu}@dsea.unipi.it

Abstract

In this paper a new method is described that allows estimating the 3d shape of defects identified in guided wave signals that were acquired with a magnetostrictive type sensor. The method is based on the evaluation of flexural components extracted from data sets acquired by a multitude of sensors distributed around the pipe circumference in a "collar" type configuration. In addition, to prove its efficiency, the method will be applied to a large number of simulated data and will finally be tested on signals acquired experimentally on real pipes with artificial defects.

Key words: guided wave, defect characterization, monitoring, pipeline, magnetostrictive

1. Background

The Guided Wave NDT technique (GW-NDT) allows the assessment [1] of the integrity of pipelines that are not accessible to classical means of non-destructive testing like bulk ultrasound, x-ray, MFL or eddy current for being buried or coated with protective or thermal insulation. Ultrasonic Guided Waves are generated by a transducer applied locally around the inspected pipe circumference and propagate along the longitudinal direction of the pipe. If defects are present like corrosion, metal loss or even cracks, a reflected wave is generated and detected by the same transducer. In this way, tens of meters of pipeline can be inspected from a single sensor position. Moreover, the technique is volumetric because of the wave propagating within the entire volume of the pipe-wall. This is why, both internal and external defects can be revealed. However, Guided Wave NDT is still considered a screening technique for being unable by itself to precisely characterise defects in terms of geometry. For this reason, a usual Guided Wave inspection is followed by detailed tests in the areas indicated by the screening. The follow-up inspection is performed with localized NDT techniques (visual, ultrasound, eddy current etc).
Prevention of corrosion effects is one of the most important issues not only within industrial plants, but also in the oil and gas distribution network, which makes the field of application of GW-NDT notably vast [2], [3].
The advantages derived from the application of GW-NDT can be outlined when considering safety - GW-NDT can identify presence of defects before a pipe failure may take place; and costs - it allows the inspection of large pipe areas in relatively short times compared to the conventional NDT techniques, with no need to stop the production cycle or fuel distribution.

2. Instruments and Methods

2.1. GW inspection and monitoring using conventional magnetostrictive sensors

An inspection system based on the Ultrasonic Guided Wave technology has been developed by the South West Research Institute from San Antonio, Tx, USA. Figure 1 shows basic constituents of the system, including the transducer itself composed of two elements:

- an electro-magnetic element made of a system of coils wrapped around the pipe; the coils generate an alternate magnetic field in the transmission phase (Tx) while inductively acquire magnetic flux variations when acting as a receiver (Rx).
- A magneto-mechanical element consisting in magnetostrictive strips directly bonded to the wall of the inspected pipe; the strips (made of ferromagnetic material) vibrate under the influence of the alternate magnetic field, generating a mechanical wave (torsional mode T(0,1)) that in turn, is transmitted to the pipe-wall [4]; in receiver mode, the strips generate an alternate field when subject to vibration.

Fig.1 MsS 2020D Inspection System and transducer.

An extensive experimental campaign was conducted on dismounted pipes in laboratory as well as on real in-service pipelines using the Guided Wave instrument MsS2020D. The results obtained and described in detail in [5], [6] and [7] can confirm the typical advantages of the GW-NDT technique:

- provides fast and reliable information over long stretches of pipeline;
- requires minimal preparation;
- allows the inspection in remote and inaccessible areas;
- reduces the costs of quantitative inspection, as it indicates precisely the critical areas that need follow-up inspection;
- brings a notable contribution to the increase in the inspection efficiency.

The advantages described above are generally characteristics of the technique independently on the GW system used, being valid for both piezoelectric and magnetostrictive systems.

2.2. Particular applications suitable to magnetostrictive GW systems

A. Low-cost inspection of large OD pipes

The magnetostrictive system was applied to the inspection of pipes with diameters ranging from 2" to 48 ". In addition, a cylindrical water tank with a 2m diameter has been inspected successfully (Fig.2).

Fig.2 Water tank inspection

B. Long-term monitoring of coated pipelines

The test shown in Fig. 3 relates to a 10" pipe, 12m long with an FBE coating proved that the results are stable when switching between the following two situations:

1) Signal acquisition with the transducer coils placed in contact with the ferromagnetic strips previously bonded on the pipe;
2) Signal acquisition with the ferromagnetic strips covered by insulation and the transducer coils placed above the insulation, in correspondence of the strips.

Fig.3. Monitoring of coated pipes: test procedure and results

The result suggests that the following procedure can be applied when inspecting coating pipes:

- the coating is removed over a stretch of a few tens of centimetres;
- the ferromagnetic strips are placed on and in contact with the pipe-wall;
- the coating is placed back;
- the transducer coils are placed over the coating in correspondence of the strips and the first signal acquisition is made;
- the ferromagnetic strips are left in place for further acquisitions to be made in order to monitor the state of integrity of the pipe over time.

C. Monitoring of pipes used in cryogenic industry

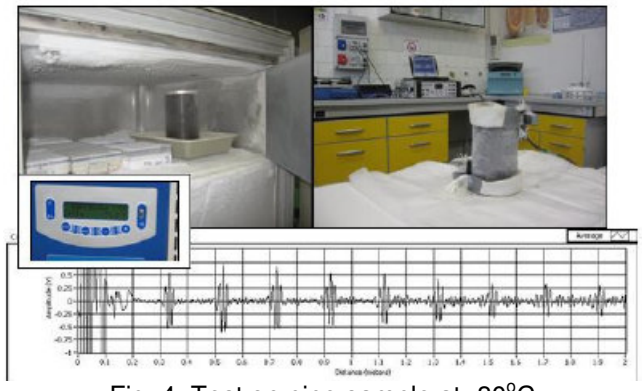
Fig. 4. Test on pipe sample at -80°C

Considering their basic components, magnetostrictive sensors can be used at extremely low temperatures. To prove it, several tests have been conducted on a sample pipe cooled down to -80°C in a first phase and to -196°C when immersed into liquid nitrogen in the second phase. During the experiments sensor components resisted to the extreme conditions and the acquired signal was stable over time and had good signal-to-noise ratio (Fig.4). the fact that the sensor can be installed permanently under the coating, makes the sensor a good candidate for applications in the refrigeration systems, liquefied gasses industry, and LNG plants.

D. Magnetostrictive collar

Methods that apply guided wave technology for pipeline screening purposes have seen important technological improvements in the past years, gaining more and more popularity amongst industrial users. Existing commercial instruments use piezoelectricity or magnetostriction to generate guided acoustic waves in pipelines and for their further detection. Transduction principle, transducing material, geometrical configuration and spatial distribution of the transduction elements are only some of the main differences between the two technologies that make them suitable to different particular applications. Piezoelectric instruments (PZT) that are commercially available use multi-element Tx/Rx transducer collar, while magnetostrictive commercial systems (MCS) use a continuous Tx/Rx transducer strip bonded around the pipe circumference. These two configurations bring significant differences between the two systems in what wave generation and acquisition is concerned.

It is well known that a multitude of guided-wave modes are generated in pipes that are inspected using guided-wave technology. For instance symmetrical wave modes like longitudinal or torsional are generated by the guided-wave instrumentation and echoes are evaluated to detect discontinuities

in the pipe-wall like defects and/or imperfections. On the other hand, the presence of asymmetrical wave modes like flexural modes indicates the presence of asymmetrical discontinuities that can be assimilated to defects. The multi-element transducer collar configuration of the PZT systems allows a better control of the wave generation process like for instance the focalization of the transmitted guided wave for a better identification and characterisation of discontinuities. However, in some cases, depending on the number of elements distributed around the pipe circumference, asymmetrical wave modes can be generated. In the acquisition process, this configuration allows wave mode separation, thus asymmetrical modes generated by asymmetrical discontinuities (mainly defects) can be evaluated to clearly discriminate defects from the other pipe features.

In contrast, the configuration of magnetostrictive guided-wave systems can be described as a single continuous transducing element attached to the pipe and surrounding the circumference independently of the pipe size. With this configuration the generated wave mode is always symmetrical (torsional or longitudinal) and no asymmetrical modes are generated. As a drawback, less wave control can be achieved with a single channel transmitter. In the acquisition process, asymmetrical modes generated by defects can be observed with certain difficulty because of the use of a single receiver.

In [8] and [9] a new configuration for magnetostrictive systems was proposed. It uses the same continuous transducer as described earlier for the generation of symmetrical torsional waves while the acquisition system is formed of multiple acquisition elements that are uniformly distributed around the pipe circumference. In addition, the capacity of the new acquisition system to perform mode separation has been demonstrated.

The magnetostrictive collar used for data acquisition and successive mode separation is shown in Fig.5. In order to extract the flexural component in each circumferential point from the experimental data, the corresponding torsional component is needed:

$$u_{fa}(t;\Delta\theta_d,\theta_0)=\sum_{n=0}^{N}\left[u_t(P_n,t;\Delta\theta_d)\cdot\cos(\theta_n-\theta_0)\right]\Big/N \quad \text{(Eq.1)}$$

where:

u_{fa} –average circumferential displacement of the flexural component in the time instant t, reference angular position θ_0, defect angle θ_d.

u_t – local circumferential displacement of the torsional component located in circumferential point P_n, instant t, for a defect of angular extent θ_d.

The average torsional displacements are:

$$u_{ta}=\sum_{n=1}^{N}u_t(P_n,t;\Delta\theta_d)/N \quad \text{(Eq.2)}$$

Fig.5 Magnetostrictive collar and multiplexer used for the experiments

The torsional component in a specific circumferential point is acquired by the corresponding collar element. Furthermore, the flexural component is extracted using Eq.1, from the data acquired with a complete scanning over the 360 degrees of the pipe circumference. Information provided by both flexural and torsional components corresponding to a certain defect will then be used to give a 3D shape estimation of the indicated defect.

3. 3D characterization of defects from simulated data

In this section a multitude of simulated data is used to perform 3D characterization of defects. The procedure described in [8] was then applied to estimate defect's angular extent, while axial extent was estimated by performing a frequency scan and evaluating the amplitudes of the reflection generated by the defect at every tested frequency.

It was demonstrated in [9] that defect's cross-sectional area is directly related to the amplitude of the reflected average torsional wave. Knowing the cross-sectional area and defects angular extent gives the possibility to estimate the most important dimension: defect's depth.

In the simulations, several parameters were varied like pipe diameter, test frequency, distance to defects and of course defect shape: axial length, circumferential extent and radial depth.

Table 1 gives a list of simulated defects, with reference to the characteristics sketched in Fig. 6.

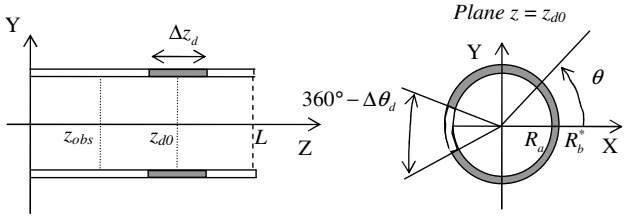

Fig. 6: defect geometry

In [8] a detailed description of defects geometry is given along with simulation parameters.

A number of 660 defects were simulated using FEM commercial software. In the next step, each defect was applied the characterisation algorithms, and the relative errors were computed.

The first parameter to be determined is the axial extent, using the amplitude-frequency relation. Next, an amplitude correction is performed to count for the interferences that are due to the distance between the two axial extremities of the defect in relation to the test wavelength. Last, the other geometrical characteristics are determined by using advanced techniques for feature recognition like support vector machines and neural networks.

Figures 7, 8 and 9 show the relative error on the prediction of defect's angular extent, cross-sectional loss and radial depth respectively. In the figures, each bar represents the number of defects whose geometry was predicted with a given relative error. For example, in the case of the angular extent error in Fig.7, about 100 defects out of a total of 660 simulated defects were characterized, obtaining a relative error close to 0% while the remaining defects presented relative errors between -10% and 10%. Similar interpretations can be given to figures 8 and 9 corresponding to errors on the cross-sectional loss and radial depth respectively.

Table 1: Simmulation parameters

Parameter		***Values***
Pipe diameter		20, 30.6(cm)
Wave frequency		16, 20, 24, 28, 32, 36, 40 (kHz)
Defect	Axial length	0.6, 1.2, 1.8, 2.4 …….20, 40(cm)
	Angular extent	10, 20, 30, …..360 (degrees)
	Radial depth	10, 30, 50, 70 (% of total wall thickness)

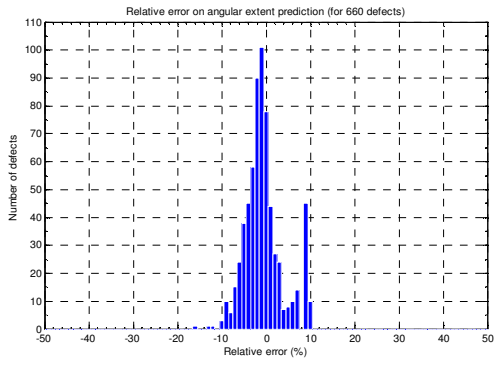

Fig. 7 Prediction error: angular extent

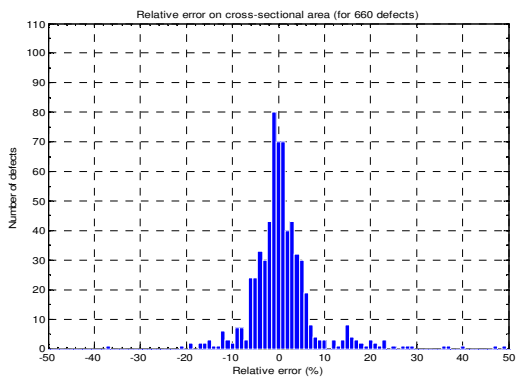

Fig.8 Prediction error: cross-sectional loss

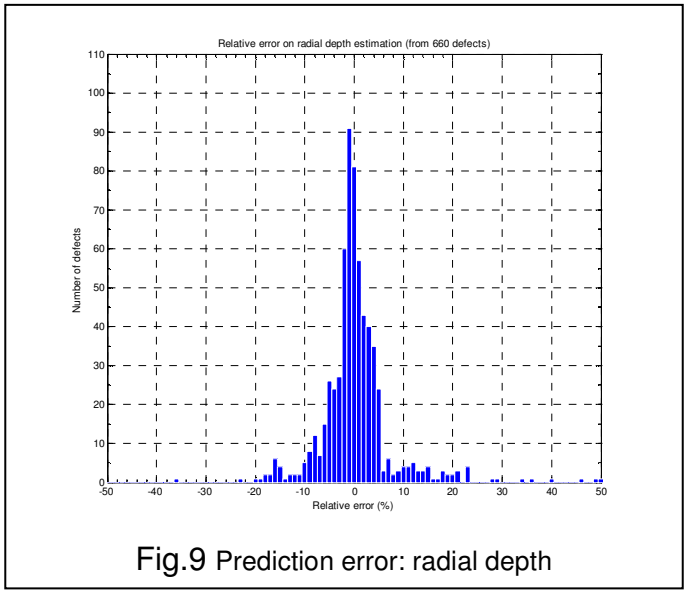

Fig.9 Prediction error: radial depth

Results of the characterization of simulated defects show that recognition algorithms perform well in the case of noise-free signals although some errors are encountered in the cases of low amplitude signals that are usually reflections generated by defects with a low angular extent.

4. Experimental results

In the last phase, the procedure for the characterization of defects was evaluated by applying it to experimental signals. For this purpose several tests were performed on pipes available in laboratory but also on in-service pipelines with several artificial defects and discontinuities (welds, flanges, joints) having different geometries. Most defects were created by bonding pieces of metal to the pipe wall. This procedure allows to repeat tests multiple times on the same pipe and to precisely measure the defects. Moreover, it was proved in previous works, that a "metal gain" defect generates a similar response to guided waves as "metal-loss" defects with the same geometry.
Figure 10 describes artificial defects and their geometry, while figure 11 shows the results of the inspection of an in-service gas pipeline. In this case, for example, all the indicated discontinuities were given a 3D characterization. Some of them were classified as 25% depth, 360° (symmetrical) discontinuities (welds) while others were classified as being asymmetrical discontinuities with various angles and depths (artificial defects). In figure 11 defects are highlighted by the high amplitude flexurals (red line in the lower graph or the high intensities in the colormap) while welds in correspondence of the high torsional/flexural ratio (high amplitude black line, low amplitude red line).

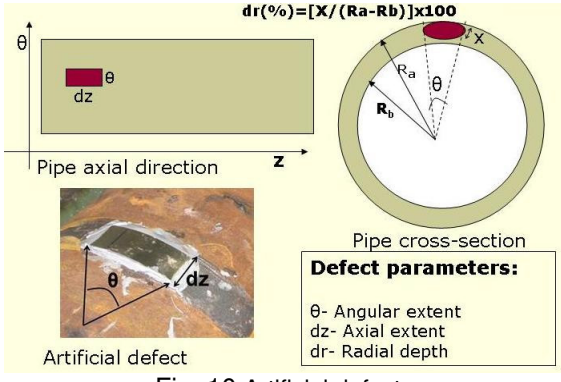

Fig. 10 Artificial defects

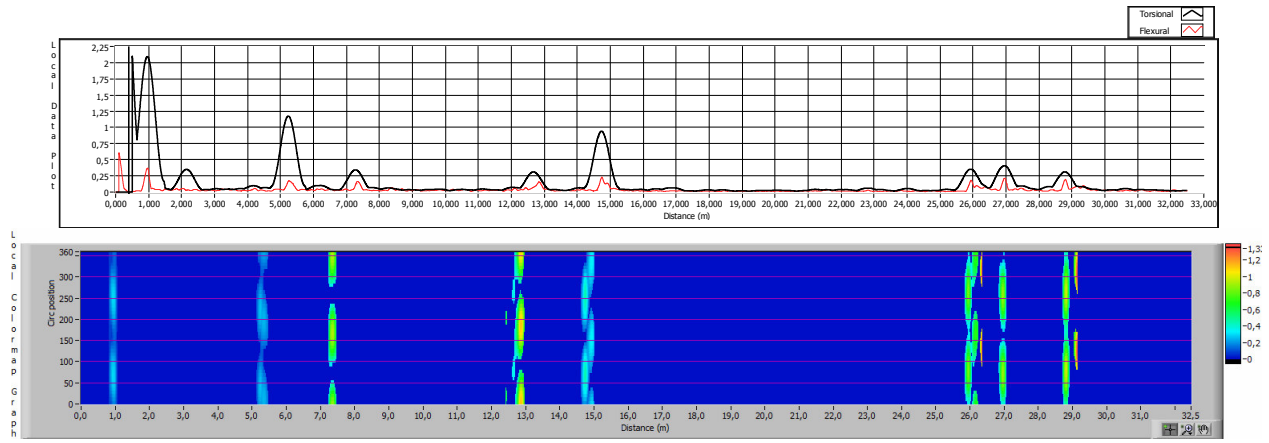

Fig.11 Results of inspection on a gas pipeline while in service-
up: torsional component (black line) and flexural component (red line)
down: colormap flexural of the flexural components: high amplitude flexural => high asymmetry

For this paper a number of 29 discontinuities with geometries randomly distributed were characterized for their angular extent, cross-sectional loss and radial depth (dθ, dS and dr respectively) and the relative errors of prediction were computed.
For a better understanding of the results, two graphical representations were used.
Figures, 12, 14 and 16 represent in the form of scatter plots the values of defect dimensions: real versus predicted. For example, in Fig. 12, a real angular extent of 110 degrees was predicted as being of 210 degrees. In the case of a perfect prediction method/algorithm all the stars would be on the line between the origin of the axes and the point of coordinates (360, 360) (bisector). Similar interpretations are valid for Fig. 14 and Fig. 16.
Concerning figures 13, 15 and 17, like in the case of simulated defects, each bar represents the number of defects whose geometry was predicted with a given relative error. To give an example, in Fig.13 the angular extent of 2 out of 29 defects was predicted with a 20% relative error, while 8 of them were predicted with relative errors of 5%.
In the following the results for the prediction of each defect parameter are explained.

a) Prediction of the angular extent (dθ)

The angular extent was predicted by evaluating the flexural response of each discontinuity with respect to the torsional and using it as an input for classification algorithms like neural networks and support vector machines. Fig 12 indicates that most errors are in the area of small angles (less than 45^{o}) and for large angles (more than 300^{o} or welds). In the first case the large errors appear because of the signal amplitudes (both torsional and flexural) that is close to the noise level. In the case of large angles, errors are due to the noise overlapping the flexural component, thus increasing it above the minimum level that should exist in the case of symmetrical discontinuities. Figure 13 shows the distribution of errors for the measured 29 defects. Most of them (20/29) have relative errors between 0 and 10%, while the others correspond to relatively small angle defects or symmetrical discontinuities as explained above.

b) Cross-sectional loss (dS)

This is the information that usually NDT instruments/software has to provide to the operators when discontinuities are indicated by the inspection results. Knowing cross-sectional wall loss is of crucial importance for the pipe operators, so they can understand the state of the pipe integrity and decide the future actions to be taken.

The cross-sectional wall loss was estimated by computing the ratio between the maximum amplitude of the transmitted wave and the maximum amplitude of the reflected wave after applying the correction for the interference due to the defect axial length. Figures 14 and 15 show small relative errors for all the 29 measured discontinuities, most of them concentrated between -10% and 10% with respect to the total pipe-wall cross-section.

c) Radial depth (dr)

In this work, the radial depth was computed after finding the other two parameters - dθ and dS- solving eq.3:

*pi*x^2-2*pi*R*x+dS*360/dθ =0 (Eq.3)*

and dr=(x/(R-r))*100;
where dθ- angular extent;
R, r – external and internal pipe radius respectively;
dS – cross-sectional wall loss.

Figures 16 and 17 show the results and the errors on the prediction of radial depth for all the 29 discontinuities. It can be noted that the relative errors for the prediction of this parameter increase, especially for the cases of small angle defects or small cross-sectional loss. This result can be explained with the link between the radial depth and the other two parameters: small prediction errors over the angular extent and/or on the cross-sectional loss will generate important errors on the prediction of the radial depth. However, even in this case, the errors of prediction are concentrated between -10% and +10% for most discontinuities (22/29) while the rest of them show prediction errors which are around 60%.

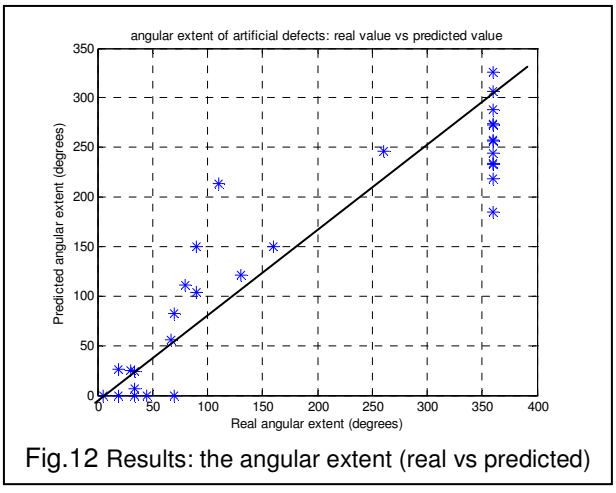

Fig.12 Results: the angular extent (real vs predicted)

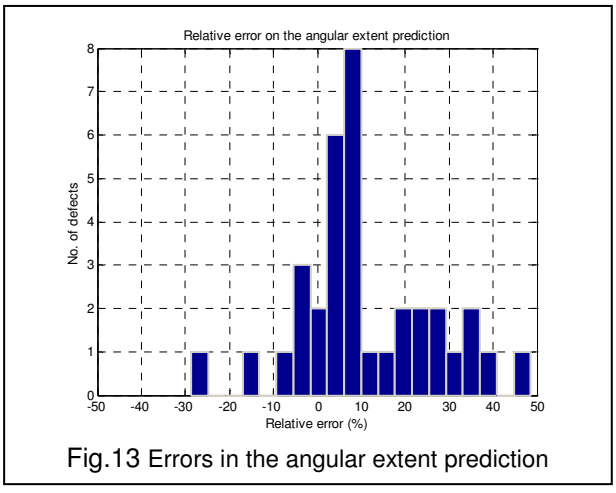

Fig.13 Errors in the angular extent prediction

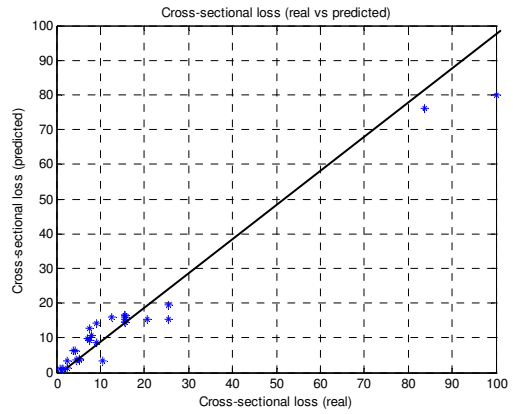

Fig.14 Results: cross-sectional loss (real vs predicted)

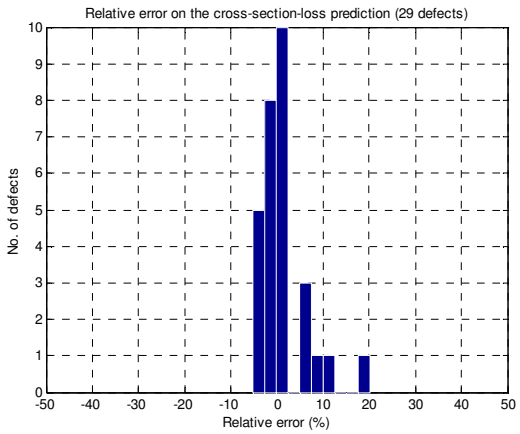

Fig.15 Errors in the cross-sectional loss prediction

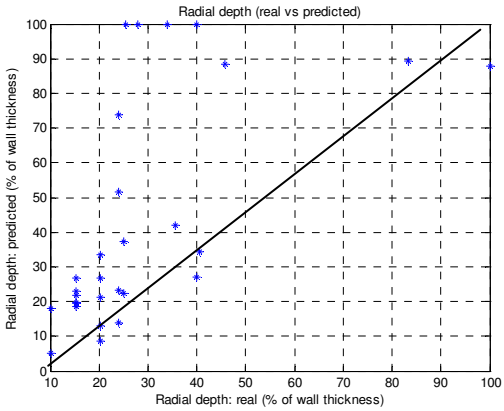

Fig.16 Results: radial depth (real vs predicted)

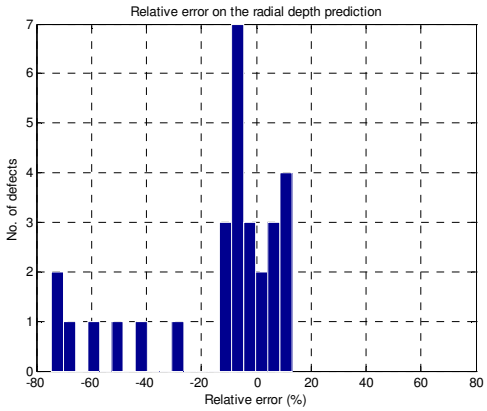

Fig.17 Errors in the radial depth prediction

5. Conclusions and future work

This paper described a multitude of tests to assess the possibility of 3d characterizing defects in pipes by using a multi element magnetostrictive collar and advanced feature recognition algorithms like neural networks. The large number of simulated defects allowed the elaboration and the evaluation of algorithms and methods capable to estimate defect's size and geometry. Furthermore, a series of experimental tests were performed using a new guided wave sensor magnetostrictive collar and artificial defects as well as discontinuities normally present on pipelines. Even though the tested discontinuities were characterized with reasonable prediction errors, a much larger number of real pipeline defects have to be tested and more experience is needed in order to make a complete evaluation of the presented methods and algorithms.

6. References

[1] P. Mudge and P. Catton, "Monitoring of Engineering Assets using Ultrasonic Guided Waves", TWI, Cambridge, UK, 9th European Conference on NDT, Berlin, Germany, September 25-29 2006.

[2] D.N. Alleyene, B. Pavlakovic, "Rapid Long Range Inspection of Chemical Plant Pipework Using Guided Waves", 15th WCNDT, Rome, 2000.

[3] P. Cawley, D. Alleyene, "Practical Long Range Guided Wave Inspection – Managing Complexity", Review of Quantitative Nondestructive Evaluation, Vol. 22, 2003.

[4] H. Kwun, K.A. Bartels, “Magnetostrictive sensor technology and its applications”, Ultrasonics, vol. 36, pp. 171-178, 1998.

[5] F. Bertoncini, M. Raugi, F. Turcu, “Sviluppo e sperimentazione di un nuovo sensore magnetostrittivo per diagnostica e monitoraggio ad onde guidate di condutture non accessibili”, AIPnD 2007, Milano, 2007.

[6] G. Acciani, F. Bertoncini, G. Brunetti, G. Fornarelli, M. Raugi, F. Turcu, “Long Range Guided Wave Inspection of Pipelines by a New Local Magnetostrictive Transducer”, Proceedings 2007 IEEE International Ultrasonics Symposium, New York, USA, 2007.

[7] F. Bertoncini, M. Raugi, F. Turcu, “Pipeline long-range inspection and monitoring by an innovative magnetic collar for magnetostrictive guided-wave systems”, NDT.net –The e-Journal of Nondestructive Testing, December 2008.

[8] F. Bertoncini, C. Oprea, M. Raugi, F. Turcu, “Defect identification by flexural component evaluation in guided wave monitoring of pipework using a magnetostrictive sensor”, The e-Journal of Nondestructive Testing, 2009.

[9] F. Turcu, “Guided Wave-NDT: Advanced sensors for pipeline monitoring”, VDM Verlag, vol1, pp. 1-130.